Characterization of films of polypropylene blended with an alicyclic oligomer through oxygen permeation measurements

Bruno Marcandalli
Stazione Sperimentale per la Seta, Via G. Colombo 81, I-20133 Milano, Italy

and Giovanni Testa and Alberto Seves
Stazione Sperimentale per la Cellulosa, Carta e Fibre Tessili Vegetali ed Artificiali, Piazza Leonardo da Vinci 26, I-20133 Milano, Italy

and Ezio Martuscelli*
Istituto di Ricerche su Tecnologie dei Polimeri, Via Toiano 6, I-80072 Arco Felice NA, Italy
(Received 1 December 1991; revised 7 August 1992)

Oxygen permeation through films of pure poly(propylene) (iPP) and iPP blended with a fully saturated alicyclic hydrocarbon resin (IST), obtained by oligomerization of indonaphthene, α-methylstyrene and vinyltoluene, was studied as a function of temperature and weight fraction of the two components. Increasing IST content lowers oxygen permeability and increases the glass transition temperature of the polymer blends. Annealing for 2 min at 375 K was shown to transform completely the smectic phase in the α crystalline form, while annealing for 10 min at 393 or 403 K induces a marked increase in crystallinity and in effective oxygen permeability per unit of amorphous component, P_a. This experimental behaviour may be explained by the formation of microvoids; the increase in microporosity modifies the mechanism of the permeation process.

(Keywords: film; polypropylene; blend; alicyclic oligomer; oxygen permeation)

INTRODUCTION

The permeation of gases through polymer films is determined by the diffusion and sorption properties involved. These properties are strongly affected by changes in the polymer matrix structure, i.e. crystallinity, phase morphology, crosslinking, porosity, free-volume distribution, chemical interactions, etc. Therefore, permeation measurements represent a useful tool for the study of polymer morphology, while knowledge of the structure–transport relationship clearly has important implications for application purposes.

In previous papers the transport of oxygen through homogeneous blends of isotactic polypropylene (iPP) and hydrogenated oligocyclopentadiene (HOCP) was studied as a function of the weight fraction of the two components, temperature and thermal history of the samples[1]. This paper extends that work by reporting on oxygen permeation measurements for blends of iPP and a fully saturated alicyclic hydrocarbon amorphous resin (IST) obtained by oligomerization of indonaphthene, α-methylstyrene and vinyltoluene.

Previous results have shown that iPP/IST blends have physical characteristics fundamentally analogous to iPP/HOCP blends[2–4]. In both cases isothermally crystallized films are completely filled with spherulites and no segregation can be observed in a wide range of concentrations; a single glass transition temperature T_g, the value of which depends on composition, is always found; Flory–Huggins parameters are negative and close to zero. These results suggest that iPP and IST are miscible in the amorphous phase of the blend, where they form a single homogeneous phase. In the melt, complete miscibility has been observed up to a weight fraction of 50% of IST.

In this paper oxygen permeation through iPP/IST films has been studied as a function of composition and temperature. Moreover, data are reported on the effect of thermal treatments on transport properties of plain iPP and iPP/IST blends.

EXPERIMENTAL

Materials

Binary blends of iPP (Moplen TS 30S, M_w 300 000, Montedison) and IST (Arkon P-140, M_w 860, Arakawa Chemical) were prepared by mixing the components in an extruder at 513 K with iPP/IST weight fractions of 90/10 and 80/20. Films of plain iPP and iPP/IST blends were extruded at 553 K and quenched in a cold water stream. The isotropic films obtained are not completely amorphous but are characterized by a smectic form. Permeation measurements were carried out on these

* To whom correspondence should be addressed

0032-3861/93/102202-06

quenched films and on films (free to shrink) subjected to various isothermal treatments: (i) 375 K for 2 min; (ii) 393 K for 2 min; (iii) 393 K for 10 min; (iv) 403 K for 10 min. All samples were characterized by various techniques as described in the following subsections.

Density measurements

Densities were measured at 298.2 ± 0.2 K by floating the samples in water–ethanol mixtures. The mass crystallinity, α_{cr}, of the samples was obtained from the measured density, ρ_x, solving the following equation system:

$$1/\rho_x = \alpha_{cr}/\rho_{cr} + \alpha_{am}/\rho_{am} + \alpha_{IST}/\rho_{IST}$$
$$\alpha_{cr} + \alpha_{am} + \alpha_{IST} = 1 \quad (1)$$

where the crystalline and amorphous components in iPP have been given the ideal values for the perfect crystal, ρ_{cr}, and fully relaxed amorphous material, ρ_{am}, i.e. 0.936 and 0.850 g cm^{-1} respectively[5], and $\rho_{IST} = 0.998$ g cm^{-3} (ref. 4) is the density of the amorphous non-crystallizable component α_{IST}. Amorphous and crystalline fractions of films are reported in *Table 1*.

Differential scanning calorimetry

The apparatus used for the measurements was a DSC-4/Thermal Analysis Data Station (TADS, Perkin–Elmer). Samples of about 5 mg were heated from 263 to 453 K at a scanning rate of 10 K min^{-1}. The apparent enthalpies of fusion were calculated from the areas of the endothermic peaks. Glass transition temperatures of iPP and the various blends studied were measured by d.s.c. scanning from 230 to 353 K and heating the samples (about 15 mg) at different rates of 20 and 40 K min^{-1}.

The crystalline and amorphous weight fractions (α_{cr} and α_{am}, respectively) were calculated as follows:

$$\alpha_{cr} = \Delta H^*/\Delta H_{iPP} \quad (2)$$

$$\alpha_{am} = (1 - \alpha_{cr}) \quad (3)$$

where ΔH_{iPP} (44 cal g^{-1}) is the heat of fusion per gram of fully crystalline iPP and ΔH^* is the apparent enthalpy of fusion of pure iPP and/or the blends studied here.

Crystalline fractions obtained through d.s.c. measurements are collected in *Table 1*, together with the relevant glass transition temperatures.

Wide angle X-ray scattering

Wide angle X-ray scattering (WAXS) data were obtained by means of a Siemens D-500 diffractometer equipped with a Siemens FK 60-10, 2000 W Cu tube with a scanning rate of 10 min per degree (2θ). The samples were mounted on a specimen carrier with a rotational speed of 30 rev min^{-1}.

Permeation measurements

The design and operation of the apparatus used for oxygen transport measurements have been described in detail elsewhere[6]. The permeation cell operates according to the so-called dynamic diffusion experiment[7], which, in principle, allows the determination of permeabilities and diffusivities in a single experimental run. The sample is placed between the two halves constituting the cells, so forming two compartments, which are first thoroughly flushed out with helium in order to remove all traces of oxygen present in the cell and in the sample itself. The experiment starts when a constant flux of oxygen is introduced into one of the chambers; the gas permeated through the film is collected by a helium stream and carried to a gas chromatograph. The permeation rates measured under the final steady-state conditions allow the determination of the permeability coefficient. The experimental deviations in the permeability coefficients were about 10%.

Table 1 Densities (ρ), crystalline and amorphous weight fractions (α_{cr} and α_{am}, respectively) and glass transition temperatures (T_g) of films of pure iPP and iPP/IST blends

iPP/IST weight fraction	Treatment[a]	ρ (g cm^{-3})	α_{cr}	α_{am}[b]	T_g (K)
100/0	q	0.888	0.47[c] (0.49)[d]	0.53	259.2
	a_1	0.898	0.58[c]	0.42	
	a_2	0.903	0.64[c]	0.36	
	a_3	0.910	0.72[c]	0.28	
	a_4	0.912	0.74[c]	0.26	
90/10	q	0.900	0.44[c] (0.44)[d]	0.56	270.9
	a_1	0.914	0.60[c]	0.40	
	a_4	0.920	0.67[c]	0.33	
80/20	q	0.911	0.41[c] (0.40)[d]	0.59	279.6
	a_1	0.923	0.54[c]	0.46	
	a_4	0.943	0.75[c]	0.25	

[a] q, quenched samples; a_1, samples annealed for 2 min at 375 K; a_2, samples annealed for 2 min at 393 K; a_3, samples annealed for 10 min at 393 K; a_4, samples annealed for 10 min at 403 K

[b] α_{am} represents: in the case of pure iPP, the amorphous weight fraction; in the blends, the amorphous fraction of iPP and non-crystallizable component

[c] From density measurements

[d] From d.s.c. measurements

RESULTS AND DISCUSSION

X-ray scattering and d.s.c. data show no marked differences between iPP/IST and iPP/HOCP blends described in a previous paper[1]. In particular, two broad peaks in WAXS scans at $2\theta = 14.8°$ and 21.5° reveal the presence of a liquid-crystalline ('smectic') form[8] in the samples of iPP and iPP/IST blends quenched in the cold water stream; the smectic phase disappears upon annealing, as shown by *Figure 1*.

The same conclusions may be drawn from d.s.c. experiments; the thermograms reported in *Figure 2* show a small but broad peak, centred at ca. 368 K and extending from 323 to 383 K, which can be attributed to the transformation from smectic to monoclinic α-crystalline form. Here, again, annealing at temperatures up to 375 K decreases the area of the exothermic peak, which finally disappears for longer annealing times and/or higher temperature treatments. Annealing for 2 min at 375 K was found to be sufficient to transform completely the smectic phase into α-crystalline form.

Experimental oxygen permeabilities, P, of films of iPP/IST blends, quenched in a cold water stream and annealed in different ways, are collected in *Table 2*, while *Table 3* reports permeability values of quenched and annealed samples of pure iPP. The measurements were carried out in the temperature range of 263–323 K.

The temperature dependence of P is illustrated by *Figure 3*, where plots of $-\ln P$ vs. T^{-1} are shown for some samples, T being the absolute temperature. The plots are linear and the data can be represented by

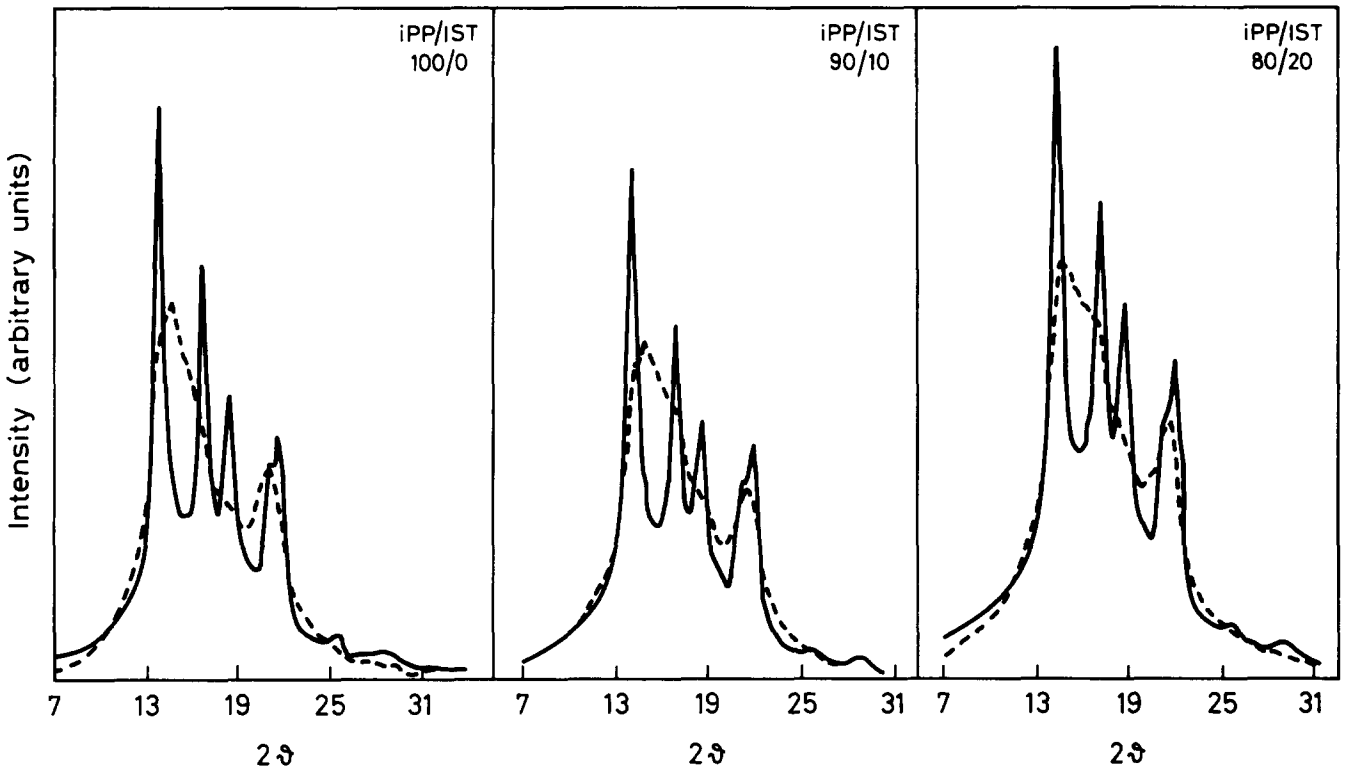

Figure 1 Wide angle X-ray diffraction of pure iPP and iPP/IST blends: full curve, annealed samples; broken curve, quenched samples

Table 2 Oxygen permeabilities (P) through films of iPP/IST blends (90/10 and 80/20 w/w) at different temperatures, T

T(K)	$P \times 10^{10}$ (cm³(STP) cm cm^{-2} cmHg^{-1} s^{-1})					
	90/10			80/20		
	q[a]	a_1	a_4	q	a_1	a_4
273.2	0.19	0.21	0.28	–	–	–
278.2	0.28	0.29	0.38	–	–	–
283.2	0.38	0.40	0.49	0.31	0.35	0.41
293.2	0.73	0.71	0.80	0.62	0.64	0.68
303.2	1.32	1.22	1.28	1.16	1.1	1.08
313.2	2.31	2.01	1.99	2.11	1.84	1.66
323.2	3.90	3.24	3.0	3.69	2.99	2.49

[a] See footnote to *Table 1*

Table 3 Oxygen permeabilities (P) at different temperatures, T, through quenched and annealed films of plain iPP

T(K)	$P \times 10^{10}$ (cm³(STP) cm cm^{-2} cmHg^{-1} s^{-1})				
	q[a]	a_1	a_2	a_3	a_4
263.2	0.15	0.15	0.14	0.16	0.19
268.2	0.22	0.21	0.19	0.22	0.25
273.2	0.31	0.29	0.27	0.31	0.34
278.2	0.44	0.40	0.38	0.41	0.45
283.2	0.60	0.55	0.51	0.55	0.59
293.2	1.11	0.98	0.91	0.96	1.0
303.2	1.96	1.71	1.56	1.62	1.62
313.2	3.36	2.85	2.59	2.63	2.55
323.2	5.57	4.62	4.17	4.15	3.9

[a] See footnote to *Table 1*

Arrhenius-type relations of the form:

$$P = P_0 \exp(-E_p/RT) \quad (4)$$

where P_0 is a constant, E_p is the apparent energy of activation of the permeation process and R is the universal gas constant. E_p values obtained using the least-squares method applied to equation (4) are collected in *Table 4*.

A detailed analysis of the data requires some general considerations. The permeation coefficient is defined as the product $P = DS$, where S is the solubility of the gas in the polymer and D is a mean diffusion coefficient. Since both S and D generally depend in complex ways on penetrant concentration, temperature, crystallinity, crosslinking, free-volume distribution in the amorphous part of the polymer matrix, etc., P is in principle a function of the same parameters. As far as the effect of the presence of crystalline regions in the polymer is concerned, it is generally accepted that crystalline domains act as

Table 4 Apparent activation energy (E_p) for oxygen permeation through films of pure iPP and iPP/IST blends

iPP/IST weight fraction	E_p (kcal mol^{-1})				
	q[a]	a_1	a_2	a_3	a_4
100/0	10.1	9.7	9.6	9.2	8.6
90/10	10.5	9.5	–	–	8.3
80/20	11.2	9.7	–	–	8.2

[a] See footnote to *Table 1*

excluded volume for the sorption process, and it has been found, in almost every system, that the solubility is directly proportional to α_{am}, i.e.:

$$S = S_a \alpha_{am} \quad (5)$$

where S_a is the solubility of the penetrant in a completely amorphous polymer[9,10]. The dependence of D on the

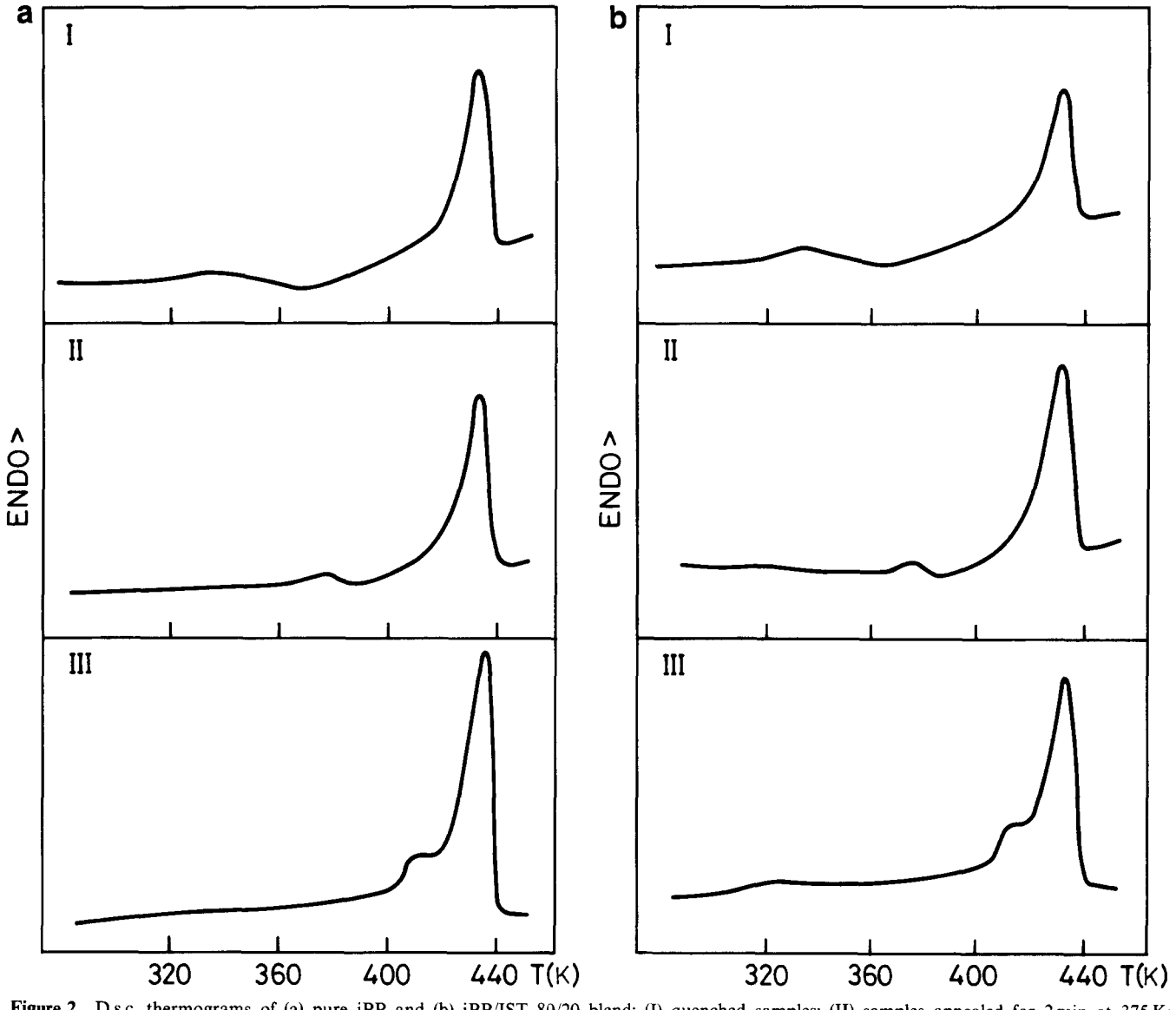

Figure 2 D.s.c. thermograms of (a) pure iPP and (b) iPP/IST 80/20 blend: (I) quenched samples; (II) samples annealed for 2 min at 375 K; (III) samples annealed for 10 min at 403 K

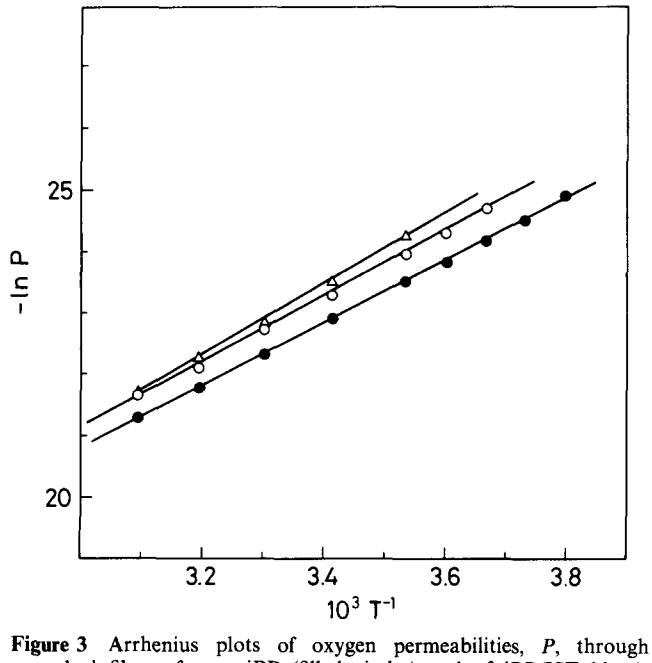

Figure 3 Arrhenius plots of oxygen permeabilities, P, through quenched films of pure iPP (filled circles) and of iPP/IST blends (open circles, iPP/IST 90/10; triangles, iPP/IST 80/20). Units of P: $cm^3(STP)\,cm\,cm^{-2}\,cmHg^{-1}\,s^{-1}$

degree of crystallinity is not so straightforward; in fact, the crystalline regions constitute effectively impermeable barriers for diffusion and increase the average path length of the permeating molecule. This effect may be accounted for empirically by the following expression:

$$D = D_a/\tau \tag{6}$$

D_a being the diffusion coefficient in a completely amorphous polymer and τ a tortuosity factor, which is a complex function of the characteristics both of the diffusing molecule and of the matrix and is generally greater than unity. Dimensions and shape of the permeating species, crosslinking, dimensions of the crystallites, presence and distribution of microvoids, etc., have been found to affect τ strongly[9].

Combining equations (5) and (6) gives:

$$P = D_a S_a \alpha_{am}/\tau \tag{7}$$

and, therefore, in an unstrained polymer, permeability is expected to increase as α_{am} increases[11]. On the contrary, in our case, addition of IST to iPP lowers the permeability even if α_{am} increases. The behaviour of iPP/IST blends is analogous to that of iPP/HOCP blends, studied previously[7]; the barrier effect imparted to iPP by addition of IST seems to be a little more marked than that observed

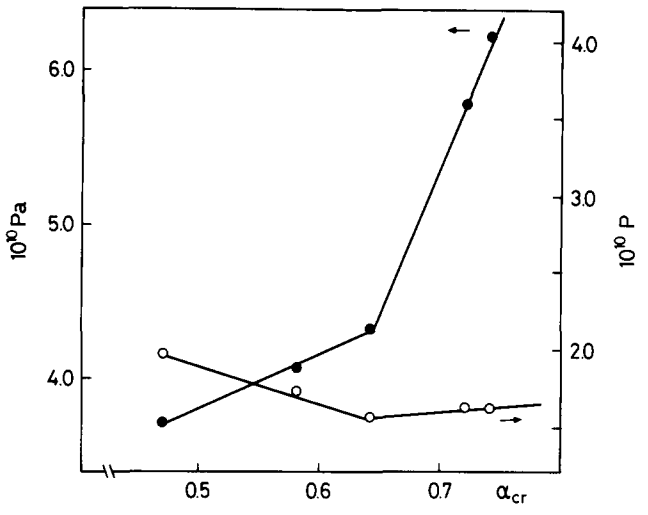

Figure 4 Oxygen permeabilities, P (open circles), and effective oxygen permeabilities, P_a (filled circles), of annealed films of pure iPP as a function of crystalline weight fraction, α_{cr}, at 303.2 K. Units of P and P_a: $cm^3(STP)\,cm\,cm^{-2}\,cmHg^{-1}\,s^{-1}$

for HOCP. This phenomenon is in line with the stronger increase of T_g brought about by IST than by HOCP, indicating a more restricted rotational mobility of chain segments.

In order to get a deeper insight into the influence of crystallinity on permeation, some samples were subjected to the thermal treatments described in the 'Experimental' section, which, as expected, bring about an increase in α_{cr} (see *Table 1*). If we take into consideration, first of all, experiments on plain iPP films, the values of P collected in *Table 3* reveal that different factors are at work in determining their permeation properties. On the basis of equation (6) we may define an effective permeability per unit of amorphous component, P_a, as:

$$P_a = P/\alpha_{am}$$

which, as a first approximation, should take into account the excluded-volume effect of the crystalline fraction.

The plots of P and P_a as a function of α_{cr} for plain iPP films are shown in *Figure 4*.

After thermal treatment of isotropic films that are free to shrink, density, crystallinity and consequently bulk volume contraction increase. The usual decrease of gas permeability when increasing crystallinities is well known.

However, in our case, after annealing, whereas the amorphous volume fraction is lower, the plot of P_a vs. α_{cr} gives a quite surprising result: in fact, P_a tends to increase.

The anomalous behaviour of P_a shows that microstructural changes are also occurring in the non-crystalline region. It is clear that permeation through the amorphous part is facilitated by annealing, especially for α_{cr} values greater than 0.64.

The films quenched in a cold water stream are not completely amorphous but are characterized by a smectic phase, which was changed into the α form when thermally treated at 375 K for 2 min.

Raising the annealing conditions progressively increases lamellar crystallite dimensions and nucleation and growth of new crystallites, and the amorphous phase will be widely distributed in small individual zones. Further thermal treatment (at 393 K or 403 K for 10 min) probably causes modification of the non-crystalline phase in the surroundings of the crystallites, so that the formation of microvoids could be favoured.

In this way a much larger quantity of gas may be trapped in the polymer, increasing solubility; moreover, the penetrating molecules may find an easier path, thus increasing further the effective permeability. These factors can overcome the barrier effect produced by the crystalline portion.

This hypothesis may be supported also by some dyeing experiments carried out previously[12]. It was found that annealing of non-amorphous poly(ethylene terephthalate) gives rise to a decrease in dye uptake, as expected as a consequence of the increased crystalline fraction, only up to a certain α_{cr}; subsequently, for greater crystallinities, an increase in the amount of dye absorbed by the polymer is observed. This phenomenon was explained by assuming an increase in porosity as a consequence of the process of crystal growth.

In the case of iPP/IST blends the dependence of the permeation coefficient on thermal treatments follows the same trend found for pure iPP films. The effect is even more marked; in fact, if we consider, for example, samples subjected to an annealing treatment of 10 min at 403 K, the ratios of the effective permeabilities of annealed and quenched samples, measured at 293.2 K, are 3.1 and 3.2 for iPP/IST 90/10 and 80/20 blends respectively, in comparison with a ratio of 2.0 found in the case of plain iPP, as may be obtained from data reported in *Table 2*. Also, the energy of activation of the permeation process was found to depend not only on sample composition but also on thermal history of the samples. While addition of IST increases E_p in the quenched samples as a consequence of the lower chain mobility, annealing reduces the activation energy, especially in the case of films containing more IST.

This experimental behaviour may be explained again by the formation of microvoids inside the polymer matrix brought about by thermal treatment. The increase in microporosity modifies the mechanism of the permeation process. In the quenched films, characterized by lower porosities, the migration of oxygen may be visualized fundamentally as a sequence of unit diffusional jumps over the potential barrier separating one position from the next. In this case the restriction induced on the rotational mobility of the chain segments by the presence of IST is the prevailing factor, and addition of IST reduces the permeation coefficients and increases the apparent activation energy. As the fraction of microvoids becomes greater, the mode of transport of a growing number of penetrating molecules changes; less energy is required to 'loosen' the structure of the polymer matrix and the overall process is likely to be better described by a model analogous to the so-called 'dual-sorption' model[13,14].

ACKNOWLEDGEMENT

This work was financially supported by Consiglio Nazionale delle Ricerche (CNR) through Progetto Finalizzato per la Chimica Fine II.

REFERENCES

1 Marcandalli, B., Testa, G., Seves, A. and Martuscelli, E. *Polymer* 1991, **32**, 3376

2 Martuscelli, E., Silvestre, C., Canetti, M., de Lalla, C., Bonfatti, A. M. and Seves, A. *Makromol. Chem.* 1989, **190**, 2615

3 Canetti, M., Bonfatti, A.M., Siciliano, A. and Seves, A. *Angew. Makromol. Chem.* 1992, **197**, 59
4 Martuscelli, E., Canetti, M. and Seves, A. *Polymer* 1989, **30**, 304
5 Van Krevelen, D. W. 'Properties of Polymers', Elsevier, New York, 1976
6 Marcandalli, B., Selli, E., Tacchi, R., Bellobono, I. R. and Leidi, G. *Desalination* 1984, **51**, 113
7 Felder, R. M. *J. Membr. Sci.* 1978, **3**, 15
8 Hsu, C. C., Geil, P. H., Miyaji, H. and Asai, K. *J. Polym. Sci. (B)* 1986, **24**, 2379
9 Sobolev, I., Meyer, J. A., Stannett, V. and Szwarc, M. *Ind. Eng. Chem.* 1957, **49**, 441
10 Michaels, A. S. and Parker, R. B. *J. Polym. Sci.* 1959, **41**, 53
11 Myers, A. W., Rogers, C. E., Stannett, V. and Szwarc, M. *TAPPI* 1958, **41**, 716
12 Vicini, L., Sadocco, P., Canetti, M., Galli, R. and Seves, A. *Acta Polym.* 1984, **35**, 588
13 Vieth, W. R., Howell, J. M. and Hsieh, J. H. *J. Membr. Sci.* 1976, **1**, 177
14 Rogers, C. E. in 'Polymer Permeability' (Ed. J. Comyn), Elsevier Applied Science, London, 1986, Ch. 2, pp. 11–73